論 文

[2179] IDENTIFICATION OF MODEL PARAMETERS OF A REINFORCED CONCRETE BRIDGE BY KALMAN FILTER THEORY

Andres W.C. ORETA* and Tada-aki TANABE*

ABSTRACT

The application of system identification to existing structures is an important step towards the aim of estimating the existing conditions and degree of damage and deterioration of structures.

In the present study, system identification using the Kalman filter method is applied to an in-situ reinforced concrete bridge to identify its modal parameters, i.e., natural frequencies and damping ratios. The free vibration response data obtained from field vibration tests is used in the identification. Results from the system identification are compared to those obtained from spectra analysis. An analysis of the numerical convergence of the parameters is discussed.

1. INTRODUCTION

The increasing importance of the problem of system identification and parameter estimation as applied to structural engineering, particularly in connection with the estimation of the existing condition of structures for the assessment of damage and deterioration, has led to the development of different system identification and parameter estimation techniques. One of the various techniques that has become increasingly popular in recent years is the Kalman filter method. The Kalman filter method has been successfully applied to linear multi-degree of freedom (MDOF) systems and to single DOF nonlinear systems. In the case of linear MDOF systems, only structures with no more than three DOF have been considered, and in most cases the response and observation data used were numerically simulated. The application of system identification using Kalman filter to in-situ structures seems lacking.

In the present study, system identification using the Kalman filter method is applied to an in-situ reinforced concrete bridge. Using an identification technique based on modal analysis, the modal parameters, i.e., natural circular frequencies and the damping ratios, are estimated.

* Department of Civil Engineering, Nagoya Univeristy

Field vibration tests are conducted to obtain data for the purpose of the identification. Results from the system identification are compared with those obtained by spectra analysis. An analysis of the numerical convergence of the parameters is also discussed.

2. MODAL EQUATIONS OF MOTION

The governing equation of motion for a multidegree of freedom linear system under free vibration is generally given by

$$\mathbf{M}\ddot{\mathbf{Z}} + \mathbf{C}\dot{\mathbf{Z}} + \mathbf{K}\mathbf{Z} = \mathbf{0}, \tag{1}$$

in which $\mathbf{M}, \mathbf{C}, \mathbf{K} = n \times n$ mass, viscous damping and stiffness matrix, respectively.

Let Φ and y be the mode-shape matrix and the generalized response vector of the system, respectively. Substituting $\mathbf{Z} = \Phi y$, Eq. (1) can be transformed into a set of uncoupled modal equations as

$$\ddot{y}_j + 2h_j\omega_j\dot{y}_j + \omega_j^2 y_j = 0, \tag{2}$$

in which h_j and ω_j are the modal damping ratio and natural circular frequency of the jth mode shape. From Eq. (2), we can derive the modal response of the ith displacement as

$$\ddot{u}_{ij} + 2h_j\omega_j\dot{u}_{ij} + \omega_j^2 u_{ij} = 0, \tag{3}$$

where $u_{ij} = \phi_{ij}y_j$, ϕ_{ij} = the element of Φ associated with the jth mode and the ith displacement. Hence, u_{ij} is the jth mode contribution to the ith displacement and for every ith displacement, we have n-set of equations of the form Eq.(3). The total ith displacement , when the effects of all the modes are taken into account is obtained by superposition as

$$\mathbf{Z}_i = u_{i1} + u_{i2} + \cdots + u_{in} \tag{4}$$

3. MODAL PARAMETER IDENTIFICATION

3.1 STATE SPACE FORMULATION

Using the following state vector defined as

$$\begin{aligned}\mathbf{X}_j &= \{\, x_{1j} \quad x_{2j} \quad x_{3j} \quad x_{4j} \quad x_{5j} \,\}^T \\ &= \{\, u_{ij} \quad \dot{u}_{ij} \quad \ddot{u}_{ij} \quad h_j \quad \omega_j \,\}^T,\end{aligned} \tag{5}$$

Eq. (3) can be transformed by using the linear acceleration method into a discrete state vector representation as

$$\mathbf{X}_j(k+1) = \begin{Bmatrix} x_{1j}(k+1) \\ x_{2j}(k+1) \\ x_{3j}(k+1) \\ x_{4j}(k+1) \\ x_{5j}(k+1) \end{Bmatrix} = \begin{Bmatrix} D_{11}x_{1j}(k) + D_{12}x_{2j}(k) + D_{13}x_{3j}(k) \\ D_{21}x_{1j}(k) + D_{22}x_{2j}(k) + D_{23}x_{3j}(k) \\ D_{31}x_{1j}(k) + D_{32}x_{2j}(k) + D_{33}x_{3j}(k) \\ x_{4j}(k) \\ x_{5j}(k) \end{Bmatrix} = g_j(k) \tag{6}$$

where,

$$\begin{array}{ccc} D_{11} = 1 + (\Delta t)^2 D_2/6, & D_{12} = (\Delta t)(1 + (\Delta t)D_3/6), & D_{13} = (\Delta t)^2(1 + D_4/2)/3, \\ D_{21} = (\Delta t)D_2/2, & D_{22} = 1 + (\Delta t)D_3/2, & D_{23} = (\Delta t)(1 + D_4)/2, \\ D_{31} = D_2, & D_{32} = D_3, & D_{33} = D_4, \end{array}$$

with,

$$D_1 = -(1 + (\Delta t)x_{4j}(k)x_{5j}(k) + (\Delta t)^2 x_{5j}^2(k)/6)^{-1},$$

$$D_2 = D_1 x_{5j}^2(k),$$

$$D_3 = D_1(2x_{4j}(k)x_{5j}(k) + (\Delta t)x_{5j}^2(k)),$$

$$D_4 = D_1(\Delta t)x_{4j}(k)x_{5j}(k) + (\Delta t)^2 x_{5j}^2(k)/3).$$

Considering the first several predominant modes ($l < n$), the state equation of the system becomes

$$\mathbf{X} = \begin{Bmatrix} \mathbf{X}_1(k+1) \\ \mathbf{X}_2(k+1) \\ \vdots \\ \mathbf{X}_l(k+1) \end{Bmatrix} = \begin{Bmatrix} \mathbf{g}_1(k) \\ \mathbf{g}_2(k) \\ \vdots \\ \mathbf{g}_l(k) \end{Bmatrix} + \mathbf{\Gamma w}(k), \quad (7)$$

Table 1. The Kalman Filter Algorithm

(1) Store the filter state:
$\hat{x}(k/k)$ and $P(k/k)$
(2) Compute the predicted state:
$\hat{x}(k+1) = \Phi(k+1/k)\hat{x}(k/k)$
(3) Compute the predicted error covariance :
$P(k+1/k) = \Phi(k+1/k)P(k+1/k+1)\Phi^T(k+1/k)$
$+\Gamma(k+1)Q(k+1)\Gamma^T(k+1)$
(4) Compute the Kalman gain:
$K(k+1) = P(k+1/k)M^T(k+1)$
$\times[M(k+1)P(k+1/k)M^T(k+1)$
$+R(k+1)]^{-1}$
(5) Process the observation y_{k+1}:
$\hat{x}(k+1/k+1) = \hat{x}(k+1/k)$
$+K(k+1)[y_{k+1} - M(k+1)\hat{x}(k+1/k)]$
(6) Compute the filtered error covariance:
$P(k+1/k+1) = [I - K(k+1)M(k+1)]\,P(k+1/k)$
$\times[I - K(k+1)M(k+1)]^T$
$+K(k+1)R(k+1)K^T(k+1)$
(7) set $k = k+1$ and return to step (1).

where $\mathbf{w}(k)$ is the system noise vector with covariance matrix $\mathbf{Q}(k)$ and $\mathbf{\Gamma}$ is the coefficient matrix of the system noise. When the acceleration is used as observation, then the corresponding observation vector equation can be written as

$$\mathbf{Y}(k) = [0,0,1,0,0,|0,0,1,0,0,|\ldots] \begin{Bmatrix} \mathbf{X}_1(k) \\ \mathbf{X}_2(k) \\ \vdots \\ \mathbf{X}_l(k) \end{Bmatrix} + \mathbf{v}(k), \quad (8)$$

where $\mathbf{v}(k)$ is the observational noise vector with covariance matrix $\mathbf{R}(k)$

3.2 STEP-BY-STEP PARAMETER ESTIMATION

Incorporating Eq. (7) and (8) in the Kalman filter algorithm (Table 1) and using a weighted global iteration[2] for convergence purposes, the parameters $x_{4j}(= h_j)$ and $x_{5j}(= \omega_j)$ were estimated using a step-by-step approach [3] as follows:

1. First, the system is considered as a single DOF and the approximate values of the first modal quantities are obtained. This step is referred to as NM=1(free) step.
2. The second modal quantities are identified by considering the system to have two DOF. In this case, the first modal quantities obtained in step 1 are used as initial values for the elements of the state vector corresponding to the first mode and the corresponding diagonal elements of the error covariance matrix are set equal to zero. This step is referred to as NM=2(fixed) step.
3. Using the estimates of the first step and second step as initial values for the first and second modal quantities, respectively, system identification is performed again and new estimates for the first and second modal quantities are obtained. This step is referred to as NM=2(free) step.
4. Procedures similar to steps 2 and 3 are applied to the third and higher modes, as necessary.

4. VIBRATION MEASUREMENTS AND DATA ANALYSIS

A field vibration test was carried out on an existing multi-girder slab reinforced concrete bridge - the Uomi bridge (Fig. 1) which is located at Fukui prefecture. An impact vertical

force was applied at a specific node of the bridge deck using a weight-drop equipment and the vertical acceleration at selected nodes were measured using strain-gauge type accelerometers which were installed at the bottom part of the girders. From the digital data acceleration response, the power spectral density was calculated using FFT method and by peak picking, the natural frequencies and damping ratios were obtained. These calculated modal values will be used for comparison later. In this paper, the impact force was applied at node 9 (Fig. 2a) and the resulting vertical acceleration at node 2, for example, is shown in Fig. 2b.

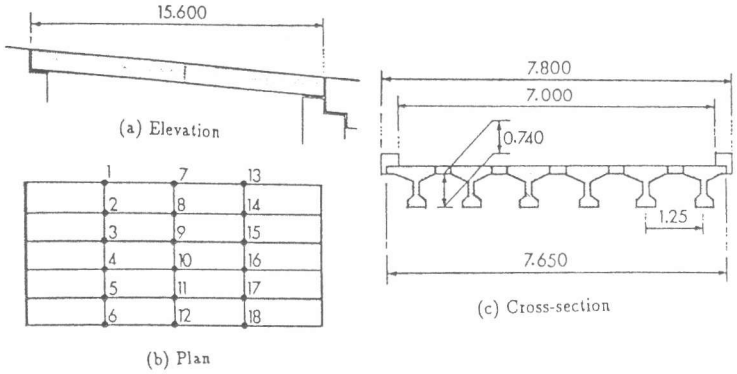

FIG. 1. Configuration of Uomi Bridge. (a) Elevation (b) Plan and Notation of Nodes (c) Cross-section

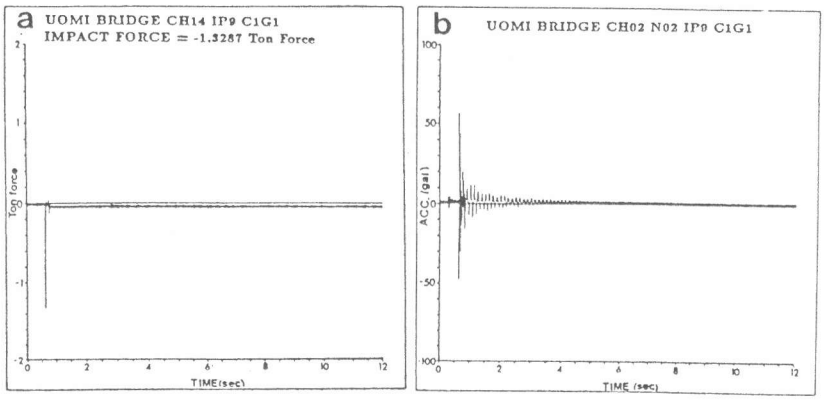

FIG. 2. Field Vibration Measurements. (a) Impact force at Node 9 (b) Vertical acceleration at Node 2

5. RESULTS OF SYSTEM IDENTIFICATION

The step by step parameter estimation procedure was applied at selected nodes of the bridge. Only the portion of the time history from 1 sec. to 4 sec. was used in the filter for free vibration analysis. A time increment of 0.001 sec. and a weight value of 100.0 in the global iteration was used. Results of the identification for nodes 2, 7, 8, 13 and 14 are shown in Table 2. For these nodes, the filter was convergent only for the first mode.

Table 2. Estimated Parameters for One-Mode Identification (h_j : damping ratio, ω_j : natural circular frequency in radians/sec.)

Node	h_1(Initial)	h_1(Estimated)	ω_1(Initial)	ω_1(Estimated)
2	0.10	0.085258	20.0	59.6004
7	0.10	0.027355	20.0	74.7669
8	0.10	0.067281	20.0	54.2946
13	0.10	0.043061	20.0	67.2518
14	0.10	0.070077	20.0	55.5611

A typical behavior of the numerical convergence of the first modal parameters for nodes 2, 7, 8, 13 and 14 is illustrated by Fig. 3. Fig. 3 shows the behavior of ω_1 at node 2. It is shown that the parameter starts to converge at the start of the 8th global iteration. Extending the identification to two modes for nodes 2, 7, 8, 13 and 14, divergent or unstable solutions resulted. For example at node 2, an unstable behavior of the parameters ω_1 and ω_2 can be seen in Fig. 4. So the identification was terminated for these nodes.

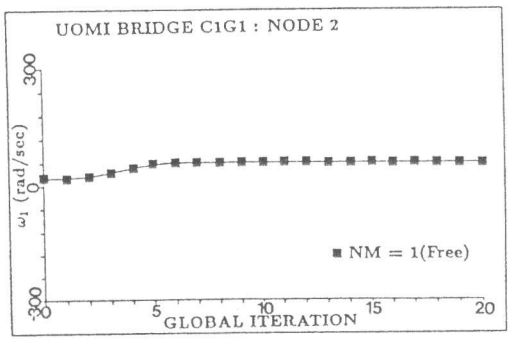

FIG. 3. Convergence of ω_1 at Node 2 NM = 1 (free) Step

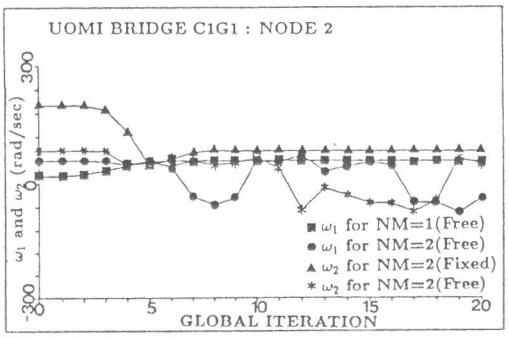

FIG. 4. Behavior of ω_1 and ω_2 at Node 2 (Two-mode Identification)

When the step-by-step identification was applied at nodes 9, 10, 15 and 16, on the otherhand, convergence extended upto the second mode. But at the three-mode identification, divergent or unreasonable results were also obtained. So the identification was also terminated for these nodes. Results of the step-by-step procedure at node 9 are shown in Table 3.

Table 3. Estimated Parameters for Two-Mode Identification at Node 9 (h_j : damping ratio, ω_j : natural circular frequency in radians/sec.)

	Initial value	Estimated values		
		NM=1(free)	NM=2(fixed)	NM=2(free)
h_1	0.10	0.036533	–	0.010295
ω_1	20.0	89.3398	–	50.5704
h_2	0.10	–	-0.118966	0.011467
ω_2	100.0	–	122.7250	132.0980

A comparison of the results from system identification with those obtained from spectra analysis is shown in Tables 4 and 5. It can be seen in these tables that the natural frequencies were reasonably estimated especially at the nodes where two-mode identification (Table 5) was applicable. The damping ratios, however, were poorly estimated.

Table 4. Comparison of Results for Nodes Identified with One-Mode Identification (h_j : damping ratio in percent, f_j : cyclic frequency in Hertz)

Node	h_1(Spec. Anal.)	h_1(Est.)	% Error	f_1(Spec. Anal.)	f_1(Est.)	% Error
2	1.3305	8.82585	540.80	8.0625	9.4857	17.65
7	1.2490	2.7355	119.02	8.0566	11.8995	47.70
8	1.2899	6.7281	421.60	8.0625	8.6412	7.18
13	1.3115	4.3061	228.33	8.0557	10.7034	32.86
14	1.2170	7.0077	475.82	8.0576	8.8428	9.74

Table 5a. Comparison of First Mode Results for Nodes Identified with Two-Mode Identification

Node	h_1(Spec. Anal.)	h_1(Est.)	% Error	f_1(Spec. Anal.)	f_1(Est.)	% Error
9	1.3325	1.0295	-22.74	8.0518	8.0485	-0.04
10	1.3206	4.6610	252.94	8.0615	7.8819	-2.22
15	1.2878	3.3981	163.87	8.0752	7.9478	-1.58
16	1.2994	3.6355	179.78	8.0664	7.9425	-1.54

Table 5b. Comparison of Second Mode Results for Nodes Identified with Two-Mode Identification

Node	h_2(Spec. Anal.)	h_2(Est.)	% Error	f_2(Spec. Anal.)	f_2(Est.)	% Error
9	1.9342	1.1467	-40.71	23.4189	21.0240	-10.23
10	1.0157	4.8230	151.76	23.4140	21.2790	-9.12
15	1.8688	3.2646	74.69	23.4499	18.9978	-18.99
16	1.9000	2.5414	33.89	23.4297	19.6645	-16.06

An interesting observation is worth noting from the study which is summarized in Table 6. If we examine the power spectra graphs for the nodes analyzed, it can be seen that for nodes where only one-mode identification was successful the value of the power spectra at f_1 was extremely dominant than that at f_2. On the otherhand, for nodes where two-mode identification was successful, the value of the power spectra at f_1 and f_2 were both dominant. It seems that the modal parameters converged upto the most significant modes only. The power spectra graphs at nodes 2 and 9 are shown in Fig. 5 for comparison. The location of the dominant values of the power spectra can be seen to lie between the range 5-10 Hz for f_1 and 20-25 Hz for f_2 as identified.

Table 6. Power Spectra (P.S.) in cm^2/sec^3
(* one-mode, ** two-mode)

Node	P.S. at f_1	P.S. at f_2
2*	3.106	0.360
7*	6.441	3.579
8*	6.789	0.4246
9**	7.500	8.476
10**	7.703	9.072
13*	2.716	2.309
14*	3.437	0.6558
15**	3.781	5.398
16**	3.867	5.380

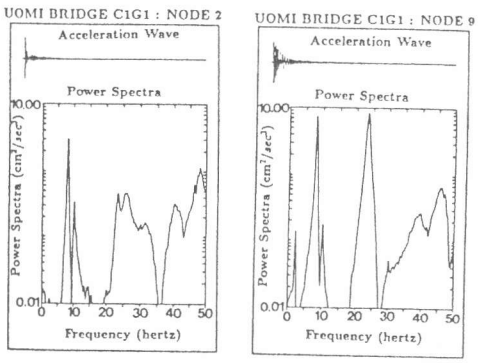

FIG. 5. Power Spectra Graphs at Selected Nodes.

6. CONCLUSION

The results of the study on the identification of natural frequencies are very encouraging. Reasonable estimates of the dominant frequencies can be identified provided that the corresponding mode is appreciably excited. Damping was poorly estimated. These relatively poor results may be due to the assumption of proportional damping which may not be true for this case. A more comprehensive research must be conducted to study the effects of sampling time, sampling length, initial values and observational noise on the identification. With an in-depth study, the consistency of the results of the identification can be verified.

REFERENCES

1) Tanabe, T. and Mizuno, T.: Study on the Identification of Dynamic Response Parameters of RC Structures, *Proc. Int. Conf. on Highrise Buildings*, 1989, pp. 499-504.

2) Hoshiya, M. and Saito, E.: Structural Identification by Extended Kalman Filter, *J.Engrg. Mechanics, ASCE*, Vol. 110, No. 12, December 1984, pp. 1757-1770.

3) Maruyama, O., Yun, C.B., Hoshiya, M. and Shinozuka, M.: Program EXKAL2 for Identification of Structural Dynamic Systems. *NCEER Technical Report*, No. NCEER-89-0014, May19, 1989